THE JOURNAL OF BIOLOGICAL CHEMISTRY VOL. 290, NO. 15, pp. 9588–9603, April 10, 2015

Di-2-pyridylketone 4,4-Dimethyl-3-thiosemicarbazone (Dp44mT) Overcomes Multidrug Resistance by a Novel Mechanism Involving the Hijacking of Lysosomal P-Glycoprotein (Pgp)*

Received for publication, December 9, 2014, and in revised form, February 24, 2015 Published, JBC Papers in Press, February 26, 2015, DOI 10.1074/jbc.M114.631283

Patric J. Jansson[1,2], **Tetsuo Yamagishi, Akanksha Arvind, Nicole Seebacher, Elaine Gutierrez, Alexandra Stacy, Sanaz Maleki, Danae Sharp, Sumit Sahni, and Des R. Richardson**[1,3]

From the Molecular Pharmacology and Pathology Program, Department of Pathology, University of Sydney, Sydney, New South Wales 2006, Australia

Background: There is a critical need for chemotherapeutics that overcome multidrug resistance (MDR).
Results: Dp44mT is transported into the lysosome by Pgp, causing lysosomal targeting of Dp44mT and resulting in enhanced cytotoxicity *in vitro* and *in vivo*.
Conclusion: Dp44mT overcomes MDR via utilization of lysosomal Pgp transport activity.
Significance: DpT thiosemicarbazones offer a new therapeutic strategy to overcome MDR via utilization of lysosomal Pgp transport activity.

Multidrug resistance (MDR) is a major obstacle in cancer treatment. More than half of human cancers express multidrug-resistant P-glycoprotein (Pgp), which correlates with a poor prognosis. Intriguingly, through an unknown mechanism, some drugs have greater activity in drug-resistant tumor cells than their drug-sensitive counterparts. Herein, we investigate how the novel anti-tumor agent di-2-pyridylketone 4,4-dimethyl-3-thiosemicarbazone (Dp44mT) overcomes MDR. Four different cell types were utilized to evaluate the effect of Pgp-potentiated lysosomal targeting of drugs to overcome MDR. To assess the mechanism of how Dp44mT overcomes drug resistance, cellular studies utilized Pgp inhibitors, Pgp silencing, lysosomotropic agents, proliferation assays, immunoblotting, a Pgp-ATPase activity assay, radiolabeled drug uptake/efflux, a rhodamine 123 retention assay, lysosomal membrane permeability assessment, and DCF (2′,7′-dichlorofluorescin) redox studies. Anti-tumor activity and selectivity of Dp44mT in Pgp-expressing, MDR cells *versus* drug-sensitive cells were studied using a BALB/c nu/nu xenograft mouse model. We demonstrate that Dp44mT is transported by the lysosomal Pgp drug pump, causing lysosomal targeting of Dp44mT and resulting in enhanced cytotoxicity in MDR cells. Lysosomal Pgp and pH were shown to be crucial for increasing Dp44mT-mediated lysosomal damage and subsequent cytotoxicity in drug-resistant cells, with Dp44mT being demonstrated to be a Pgp substrate. Indeed, Pgp-dependent lysosomal damage and cytotoxicity of Dp44mT were abrogated by Pgp inhibitors, Pgp silencing, or increasing lysosomal pH using lysosomotropic bases. *In vivo*, Dp44mT potently targeted chemotherapy-resistant human Pgp-expressing xenografted tumors relative to non-Pgp-expressing tumors in mice. This study highlights a novel Pgp hijacking strategy of the unique dipyridylthiosemicarbazone series of thiosemicarbazones that overcome MDR via utilization of lysosomal Pgp transport activity.

Success in overcoming or circumventing multidrug resistance (MDR)[4] in cancer has been challenging (1, 2). As such, MDR remains one of the major problems for effective tumor treatment (1, 2). One of the best characterized resistance mechanisms of cancer cells involves cellular efflux of chemotherapeutic drugs, such as doxorubicin (DOX; Fig. 1*A*) or vinblastine (VBL; Fig. 1*A*), through "drug pumps," including P-glycoprotein (Pgp; ABCB1) (3).

Current drug development strategies to overcome MDR place an emphasis on chemotherapeutics that are not substrates of drug efflux pumps to ensure efficient targeting of MDR cells. Moreover, attempts for over 20 years to reverse

* This work was supported by a fellowship from the Cancer Institute New South Wales and Prostate Cancer Foundation of Australia (to P. J. J.) and by a Senior Principal Research Fellowship and project grant funding from the National Health and Medical Research Council of Australia (to D. R. R.). P. J. J., T. Y., and D. R. R. are co-inventors on the patent entitled "Chemotherapy for drug-resistant cancer cells" (PCT/AU2013/001344). D. R. R. consults for Oncochel Therapeutics LLC and Pty. Ltd., the license holder of this patent application. D. R. R. is also a stakeholder in Oncochel Therapeutics LLC and Pty. Ltd.

[1] These authors contributed equally to this work as corresponding and senior authors.
[2] To whom correspondence may be addressed: Molecular Pharmacology and Pathology Program, Dept. of Pathology and Bosch Inst., Blackburn Building (D06), University of Sydney, Sydney, NSW 2006, Australia. Tel.: 61-2-9036-6547; Fax: 61-2-9351-3429; E-mail: patric.jansson@sydney.edu.au.
[3] To whom correspondence may be addressed: Molecular Pharmacology and Pathology Program, Dept. of Pathology and Bosch Inst., Blackburn Building (D06), University of Sydney, Sydney, NSW 2006, Australia. Tel.: 61-2-9036-6547; Fax: 61-2-9351-3429; E-mail: d.richardson@med.usyd.edu.au.

[4] The abbreviations used are: MDR, multidrug resistance or multidrug-resistant; Bp4eT, 2-benzoylpyridine 4-ethyl-3-thiosemicarbazone; CLQ, chloroquine; DCF, 2′,7′-dichlorofluorescin; DOX, doxorubicin; DpT, dipyridylthiosemicarbazone; Dp44mT, di-2-pyridylketone 4,4-dimethyl-3-thiosemicarbazone; Ela, Elacridar; LAMP2, lysosomal associated membrane protein-2; LMP, lysosomal membrane permeabilization; MA, methylamine; Pgp, P-glycoprotein; Rh123, rhodamine 123; ROS, reactive oxygen species; Val, valspodar; VBL, vinblastine; MTT, 3-(4,5-dimethylthiazol-2-yl)-2,5-diphenyl tetrazolium.

resistance to chemotherapeutics by using MDR modulators have not generated useful outcomes in clinical trials (4, 5). Hence, there is an increasing need to develop drugs that effectively target drug-resistant tumors.

There has been great interest in understanding the mechanism of action of agents that are more effective in drug-resistant cells than in their drug-sensitive counterparts (6, 7). One of these agents, di-2-pyridylketone 4,4-dimethyl-3-thiosemicarbazone (Dp44mT; Fig. 1*A*) (8), has been described to overcome MDR *in vitro* by an unknown mechanism (9) and to be highly effective and selective against a variety of belligerent solid human tumors *in vivo* by the intravenous and/or oral routes (9–12). An important aspect of the activity of these agents was shown to be due to their complexation with copper in lysosomes to form redox active complexes that caused lysosomal membrane permeabilization (LMP) and apoptosis (13).

The current study offers an unexplored approach describing how functional Pgp on the lysosomal membrane can be "hijacked" by agents, such as Dp44mT, to potentiate cytotoxicity in MDR cancers. Herein, we highlight the molecular mechanism and properties of agents required to overcome MDR. Moreover, the potentiated anti-cancer activity of Dp44mT in Pgp-expressing MDR cells, *versus* drug-sensitive cells, was confirmed in a human tumor in mice. Hence, this study describes a novel mechanism of action and identifies a new strategy for designing chemotherapeutics to overcome MDR by hijacking lysosomal Pgp to increase sequestration of redox active, lysosomotropic Pgp substrates into lysosomes. This effect potently enhances cytotoxicity by targeting Dp44mT to the lysosome, which is a key target of this agent, leading to LMP and death of the resistant cancer cell. This property is unique, is not found for current chemotherapeutics that are Pgp substrates, and depends on the redox activity of the Dp44mT-Cu complex. Notably, this mechanism is totally opposite to that found for standard cytotoxic drugs that are Pgp substrates, such as DOX. Indeed, in this latter case, Pgp expression results in DOX efflux and its storage in the lysosome where the organelle acts as a "safe house," preventing cytotoxicity and leading to resistance against the chemotherapeutic.

MATERIALS AND METHODS

Chemicals—DOX was purchased from Pfizer (New York, NY). VBL, methylamine (MA), NH_4Cl, $CuCl_2$, rhodamine 123 (Rh123), tetrathiomolybdate, H_2DCF, cysteine, H_2O_2, chloroquine (CLQ), MK-571, KO-143, and paclitaxel were purchased from Sigma-Aldrich. Valspodar (Val) was provided by Novartis (Basel, Switzerland). Elacridar (Ela) was from GlaxoSmithKline (London, UK). LysoTracker® Red and Lipofectamine 2000 were from Life Technologies, Inc. [^{14}C]DOX and [^{3}H]VBL were from PerkinElmer Life Sciences. Dp44mT, 2-benzoylpyridine 4-ethyl-3-thiosemicarbazone (Bp4eT), and their metal complexes were synthesized and characterized, as described previously (14–16). [^{14}C]Dp44mT was prepared by the Institute of Isotopes Ltd. (Budapest, Hungary).

Cell Culture—Human cervical carcinoma-derived KB31 cells, the small cell lung carcinoma cell line, DMS-53, the colon adenocarcinoma cell line, HCT-15, and the MCF7 and MDA-MB-231 breast carcinoma cell lines were obtained from the American Type Culture Collection (Manassas, VA), whereas VBL-resistant KBV1 cells (grown in 1 μg/ml VBL) were a gift from Dr. Maria Kavallaris (Children's Cancer Institute Australia, Sydney, Australia). The 2008 human ovarian carcinoma cell line and the paclitaxel-resistant 2008/P200 cell line (grown in 200 ng/ml paclitaxel) were from Dr. John Allen (Centenary Institute, Sydney). All cells were grown in DMEM (Life Technologies, Inc.) under standard conditions (17).

MTT Proliferation Assay—Proliferation was examined using the MTT assay and validated utilizing viable cell counts via trypan blue (13). The cells (3×10^3/well) were seeded in 96-well plates and preincubated with medium alone or Pgp inhibitors (1 μM Val or 0.1 μM Ela) or lysosomotropic agents (5 mM NH_4Cl, 1 μM CLQ, or 100 μM MA) for 30 min at 37 °C. This medium was then replaced, and the cells were incubated with DOX, VBL, Dp44mT, or Cu[Dp44mT] in the continued absence or presence of Pgp inhibitors or weak bases for 2, 24, or 72 h at 37 °C and processed (13).

Transient Pgp Silencing Using siRNA—Pgp silencing (*MDR1*-siRNA; catalog no. 4123; Life Technologies, Inc.) was performed as described (17). Briefly, the siRNA-Lipofectamine mixture (50 nM *MDR1*-siRNA and 1:400 Lipofectamine 2000) was added to the cells (at 30% confluency) and incubated for 72 h at 37 °C prior to further experiments. The effectiveness of Pgp silencing was confirmed using Western blotting and DOX and Dp44mT cytotoxicity via the MTT assay. As a relevant control, negative control siRNA with no genomic homology (Life Technologies, Inc.) was used at the same concentration as *MDR1* siRNA.

Western Blot—Standard methods were implemented for Western blotting (8) using a Pgp antibody (catalog no. P7965 clone: F4; Sigma-Aldrich). β-Actin was used as a protein loading control (catalog no. A1978; Sigma-Aldrich).

Pgp-ATPase Activity Assay—The ATPase activity of Pgp was determined using Pgp-enriched membranes and a luminescent ATP detection kit (Pgp-Glo™ ATPase assay; Promega) according to the manufacturer's instructions. Briefly, Pgp-enriched membranes (0.5 mg/ml) and Mg(II)-ATP (5 mM) were incubated in the absence or presence of sodium orthovanadate (100 μM) for 40 min at 37 °C, and ATP levels were detected as a luciferase-generated luminescent signal. Basal Pgp-ATPase activities were calculated as the difference between the ATP hydrolysis in the presence or absence of sodium orthovanadate. As relevant negative controls, the well characterized Pgp inhibitors Ela (0.1 μM) and Val (1 μM) were used to inhibit Pgp-ATPase activity (18). As a positive control, verapamil-stimulated Pgp-ATPase activity was measured in the presence of the Pgp control substrate, verapamil (200 μM) (19). The test substrates, Dp44mT, Bp4eT, or their Fe(III) and Cu(II) complexes all at 50 μM, were dissolved in DMSO (Sigma-Aldrich). The final concentration of DMSO in the assay medium was equal to or less than 0.25%. Control experiments indicated that DMSO at this concentration had no effect on ATPase activity.

Uptake/Efflux of [^{14}C]DOX, [^{3}H]Vinblastine, and [^{14}C]-Dp44mT—Cells were labeled with [^{14}C]DOX, [^{3}H]VBL, or [^{14}C]Dp44mT (all 1 μCi/ml) for 30 min at 37 °C, as described (13, 17). Drug uptake/efflux was performed in the absence or presence of Pgp inhibitors (1 μM Val or 0.1 μM Ela) or weak bases (5 mM

NH_4Cl, 100 μM MA, or 10 μM CLQ). Radioactivity was quantitated using a MicroBeta Counter (PerkinElmer Life Sciences).

Rh123 Retention Assay—Cells were preincubated with a range of concentrations (0.001–10 μM) of Dp44mT, Val, or Ela for 30 min at 37 °C, followed by incubation with Rh123 (1 μg/ml) for 15 min at 37 °C in the presence of the Pgp inhibitors or Dp44mT (17). Samples were processed and analyzed using a FACS Canto flow cytometer (BD Biosciences; 10,000 events/sample) and FlowJo software (v.7.5.5; Tree Star Inc., Ashland, OR), respectively.

Assessment of Pgp Localization and Also Lysosomal Membrane Permeability—For assessment of intracellular Pgp co-localization, cells (1×10^5 cells/ml) were grown on coverslips, followed by paraformaldehyde fixation (4%, 15 min, 20 °C) and digitonin permeabilization (100 μM, 10 min, 20 °C). Importantly, the mild detergent digitonin was utilized to specifically avoid dissolving the lysosomal membrane (20). After blocking with 5% BSA, immunofluorescence was performed by incubation (16 h, 4 °C) with FITC-conjugated anti-Pgp (1:100, catalog no. 557002; BD Biosciences) and anti-LAMP2 (1:20, catalog no. ab25631; Abcam) antibodies, and DAPI (0.5 μM; Invitrogen). In the case of the primary incubation with anti-LAMP2, this was followed by treatment (1 h, 4 °C) with Alexa Fluor-conjugated secondary antibodies (1:1000, catalog no. A-21200 and catalog no. A-21201; Invitrogen). Stained samples were examined with a Zeiss Axio Observer.Z1 microscope equipped with an AxioCam camera (Zeiss, Oberkochen, Germany) and Zeiss Axiovision co-localization software (Zeiss). Mander's overlap coefficient was determined, and scatter plots were generated using ImageJ (National Institutes of Health) from the intracellular compartments of cells.

LysoTracker® Red (Life Technologies, Inc.) and acridine orange (Sigma-Aldrich) were used to determine LMP (13). Cells were incubated with LysoTracker® Red (50 nM) or acridine orange (20 nM) for 15 min at 37 °C, washed three times with ice-cold PBS, and then incubated with Cu[Dp44mT] or Dp44mT alone (all at 25 μM) for 30 min or 24 h at 37 °C in the presence or absence of Val (1 μM) or Ela (0.1 μM). LysoTracker® Red staining of cells was detected using the microscope/software above. Acridine orange staining was analyzed using the flow cytometer above.

Pgp-dependent accumulation of Dp44mT and its effect on lysosomal stability was shown by co-incubation with the lysosomotropic weak base, CLQ. Cells (3×10^4 cells/ml) were grown on coverslips for 24 h at 37 °C and pretreated with either medium alone or CLQ (1 μM) for 30 min at 37 °C. The cells were then incubated with Cu[Dp44mT] (25 μM) in the absence or presence of CLQ for 30 min at 37 °C. Cells were fixed with methanol (100%, 15 min, 20 °C) and permeabilized with digitonin (100 μM, 10 min, 20 °C), blocked with 10% BSA (30 min at room temperature) and incubated (16 h/4 °C) with lysosomal associated membrane protein-2 (anti-LAMP2; 1:100; catalog no. ab25631; Abcam) or anti-cathepsin D (1:100; catalog no. ab72915; Abcam). This step was followed by treatment (1 h at 20 °C) with Alexa Fluor-conjugated secondary antibodies (1:1,000; catalog no. sc-2781; Santa Cruz Biotechnology and A-11008; Life Technologies, Inc.). Examination/quantitation of fluorescent stains and intracellular cathepsin D (FITC) intensity and its co-localization with LAMP2 (Texas Red) were performed using the microscope/software above.

Redox Studies: Oxidation of H_2DCF—The effect of Val (1 μM), Ela (0.1 μM), or tetrathiomolybdate (5 μM) on reactive oxygen species (ROS) generation by Cu[Dp44mT] (5 μM) was examined using H_2DCF (5 μM) in the absence of cells over 12 min at 20 °C using standard methods (13). Studies were conducted in an acetate buffer (150 mM; pH 5) containing cysteine (100 μM) to mimic lysosomal conditions (13). In these experiments, H_2O_2 (100 μM) was added to initiate ROS generation. To confirm ROS production, DMSO (10% v/v) was used, because it is an effective hydroxyl radical scavenger (21).

Tumor Xenografts in Nude Mice and Dp44mT Administration—All studies involving animals were performed in accordance with ARRIVE guidelines (22) and the University of Sydney Animal Ethics Committee. In mouse studies, sample sizes were predetermined based on previous experience with Dp44mT (9) using a minimum of six mice/group, and the experiment was replicated twice to confirm findings. KBV1 or KB31 cells (3×10^6) were suspended in Matrigel (BD Biosciences, San Jose, CA) in a 1:1 ratio and injected subcutaneously into the left (KBV1 cells) or right (KB31 cells) flank of each 7-week-old female BALB/c nu/nu mouse. After engraftment, tumor size was measured using Vernier calipers, and the tumor volumes were calculated (9). When tumor volumes reached 120 mm^3, intravenous (tail vein) vehicle or Dp44mT treatment began (day 0). The mice were randomly assigned to treatment groups, and where possible, treatment groups were blinded until statistical analysis. No animals or potential outliers were excluded from the data sets presented in this study. Dp44mT (0.1 or 0.2 mg/kg) was dissolved in 30% propylene glycol in 0.9% saline and injected intravenously over 5 consecutive days/week (9). Control mice were treated with the vehicle alone. The health of mice was assessed by monitoring weight, behavior, and comprehensive biochemical/hematological analyses (9).

Pgp Immunohistochemistry—Tumor sections were deparaffinized, rehydrated through graded ethanol solutions, and brought to distilled water. They were then subjected to heat retrieval/pressure (125 °C/30 s) and immersed in pH 9.0 Tris/EDTA buffer. After washing with distilled water, endogenous peroxidase activity was inhibited (3% H_2O_2 for 5 min), followed by a TBS/Tween wash. The primary antibody (anti-Pgp, clone EPR10363; catalog no. 170903; Abcam) was incubated at 2.5 μg/ml for 30 min at room temperature, followed by TBS/Tween washes. An IgG isotype negative control from a nonimmunized rabbit (Dako; catalog no. X0936) was matched to the concentration of the primary Pgp antibody. The complex was detected with Envision/anti-rabbit antibody (30 min at room temperature; Dako), washed with buffer, and incubated (10 min) with 3′,3-diaminobenzidene. Sections were counterstained in Harris hematoxylin and dehydrated in graded ethanols before being cleared in xylene and mounted. The images were taken using an Olympus BX53 microscope/DP72–3CCD camera (Olympus, Tokyo, Japan).

Statistics—The data were compared using two-tailed Student's t test. The results were expressed as means ± S.D. (number of experiments) or means ± S.E. (number of mice) and considered to be statistically significant when $p < 0.05$.

RESULTS

The Thiosemicarbazones, Dp44mT and Bp4eT, Exhibit a Pronounced Increase in Cytotoxicity in Cells Expressing Functional Pgp—We previously demonstrated that Dp44mT exhibits markedly increased cytotoxicity in MDR cells (9), but the mechanism involved is unknown. To initially determine whether the potentiated cytotoxicity of Dp44mT against MDR cells is Pgp-dependent, two pairs of well characterized Pgp-expressing cells and their non-Pgp-expressing counterparts were used, namely KBV1 cells (+Pgp) *versus* KB31 cells (−Pgp) (3, 7, 17) and 2008/P200A cells (+Pgp) *versus* 2008 cells (−Pgp) (17) (Fig. 1, *B–E*). In addition, two cell lines that endogenously express Pgp were also examined: DMS-53 (23) and HCT-15 cells (24) (Fig. 2). In addition, as another control, a structurally related thiosemicarbazone, 2-benzoylpyridine 4-ethyl-3-thiosemicarbazone (Bp4eT; Fig. 1*A*) (16), was also assessed for potentiated cytotoxicity in Pgp-expressing cells.

Pgp expression was marked in KBV1 and 2008/P200 cells, while being negligible in KB31 and 2008 cells (see *insets* in Fig. 1, *B* and *D*). After a 72-h incubation with the established Pgp substrates, DOX and VBL (3) (Fig. 1*A*), drug-resistant KBV1 cells (+Pgp) showed a 220- and 221-fold increase in resistance to DOX and VBL compared with KB31 cells, respectively (Fig. 1*B*).

In marked contrast, the thiosemicarbazones, Dp44mT and Bp4eT, were 31- and 6.7-fold more cytotoxic ($p < 0.001$) in drug-resistant KBV1 cells (+Pgp) compared with KB31 cells (−Pgp), respectively (Fig. 1*C*). In an opposite manner to DOX and VBL (Fig. 1*B*), Pgp inhibition by the well characterized Pgp inhibitors, Val (18) or Ela (18), led to a significant ($p < 0.001$) decrease in cytotoxicity (increased IC_{50}) of Dp44mT and Bp4eT in KBV1 cells (+Pgp; Fig. 1*C*). Notably, no significant ($p > 0.05$) change in DOX, VBL, or thiosemicarbazone cytotoxicity was observed in the presence of Pgp inhibitors in KB31 cells (−*Pgp*; Fig. 1, *B* and *C*). These observations suggested the cytotoxicity mediated by the thiosemicarbazones was Pgp-dependent. The effect of all these agents was not cell line-specific, because similar Pgp-dependent results were also obtained using 2008/P200A cells (+*Pgp*) and 2008 cells (−*Pgp*; Fig. 1, *D* and *E*).

The importance of Pgp in sensitizing cells to Dp44mT were then further substantiated by Pgp silencing (see *inset* in Fig. 1*F*) that significantly ($p < 0.001$) sensitized KBV1 cells to DOX, relative to the negative control siRNA. In contrast, KBV1 cells with Pgp silencing became significantly ($p < 0.001$) more resistant to Dp44mT relative to negative control siRNA-treated cells (Fig. 1*F*).

Similar to the observations in highly Pgp-expressing KBV1 cells and 2008/P200A cells, the DMS-53 and HCT-15 cell lines that endogenously express low to moderate Pgp levels (Fig. 2*A*) were also found to show resistance to DOX and VBL *via* Pgp (Fig. 2*B*). This was demonstrated using the Pgp inhibitors Val and Ela which decreased resistance to DOX or VBL, resulting in significantly ($p < 0.001–0.01$) lower IC_{50} values (Fig. 2*B*).

Again, as observed in KBV1 cells that highly express Pgp (Fig. 1, *B* and *C*), Dp44mT and Bp4eT were significantly ($p < 0.001–0.05$) more cytotoxic (decreased IC_{50}) in the absence of Pgp inhibitors (Val and Ela) in both DMS-53 and HCT-15 cells (Fig. 2*C*). These observations suggested the enhanced cytotoxicity mediated by these thiosemicarbazones not only is relevant in MDR cells such as KBV1 and 2008/P200 (Fig. 1, *C* and *E*) but also is important in cells expressing endogenous Pgp. Collectively, these results (Figs. 1 and 2) highlight the importance of Pgp in the potentiated toxicity exerted by Dp44mT to overcome MDR in two cell types with Pgp expression induced by prior exposure to cytotoxic drugs (*i.e.* DOX or VBL) and two cell lines with low to moderate endogenous Pgp expression.

Pgp Expression, but Not the Expression of the ABC Transporters, MRP1 and ABCG2, Affects Dp44mT Cytotoxicity—Studies were also performed to assess whether Dp44mT could potentially be transported by other well characterized ABC transporters, namely MRP1 and ABCG2 (25–27). To assess this transport activity relative to Pgp, a number of cell types were examined in cellular cytotoxicity studies measuring the IC_{50} of Dp44mT over a 24-h incubation. First, in these studies, KB31 cells were employed as a relative negative control because they do not express any of these transporters at detectable levels (Fig. 2*D*). On the other hand, as positive controls for transporter expression and activity, the following cell lines were implemented, namely: 1) KBV1 and HCT-15 cells, because they are known to express functionally active Pgp (17, 28); 2) MCF-7 cells, because they express functionally active MRP1 (29) and ABCG2 (30); and 3) MDA-MB-231 cells, because they express functionally active ABCG2 (30) (Fig. 2*D*). To assess the role of the transporters, each cell type was incubated with either the well characterized Pgp inhibitor Ela (0.2 μM) (18), the MRP1 inhibitor MK-571 (20 μM) (31), or the ABCG2 inhibitor KO-143 (2 μM) (32). The concentrations of inhibitors utilized were characterized in control experiments to be optimal in terms of inhibiting transporter activity without inducing cytotoxicity.

Because of the lack of detectable expression of Pgp, MRP1, and ABCG2 in KB31 cells (Fig. 2*D*), the relative inhibitors had no significant ($p > 0.05$) effect on the cytotoxicity of Dp44mT *versus* that observed with control medium without inhibitors in this cell line (Fig. 2*E*). On the other hand, as shown above in Figs. 1*C* and 2*C*, the Pgp inhibitor Ela markedly and significantly ($p < 0.001$) increased resistance to Dp44mT (shown by increased IC_{50} value) only in KBV1 and HCT-15 cells where Pgp is expressed (Fig. 2, *D* and *E*). In contrast to Ela, the cytotoxicity of Dp44mT was not significantly ($p > 0.05$) altered in the presence of the MRP1 inhibitor MK-571 or the ABCG2 inhibitor KO-143, in any of the cell lines (Fig. 2, *D* and *E*). Collectively, these observations suggest Dp44mT only utilizes Pgp to overcome multidrug resistance (Fig. 2, *D* and *E*).

Dp44mT and Bp4eT Are Pgp Substrates—Because the expression and function of Pgp is a prerequisite for the increased cytotoxicity of Dp44mT and Bp4eT (Figs. 1, *C*, *E*, and *F*, and 2), a Pgp-ATPase assay of a purified membrane preparation containing high levels of Pgp (33) was initially used to assess whether Dp44mT and Bp4eT interact with Pgp. The positive control verapamil (33) significantly ($p < 0.001$) increased ATPase activity ~4-fold, whereas the Pgp inhibitors, orthovanadate (33), Val, and Ela (18), significantly ($p < 0.001$) decreased the ATPase activity ≥5-fold relative to the basal level

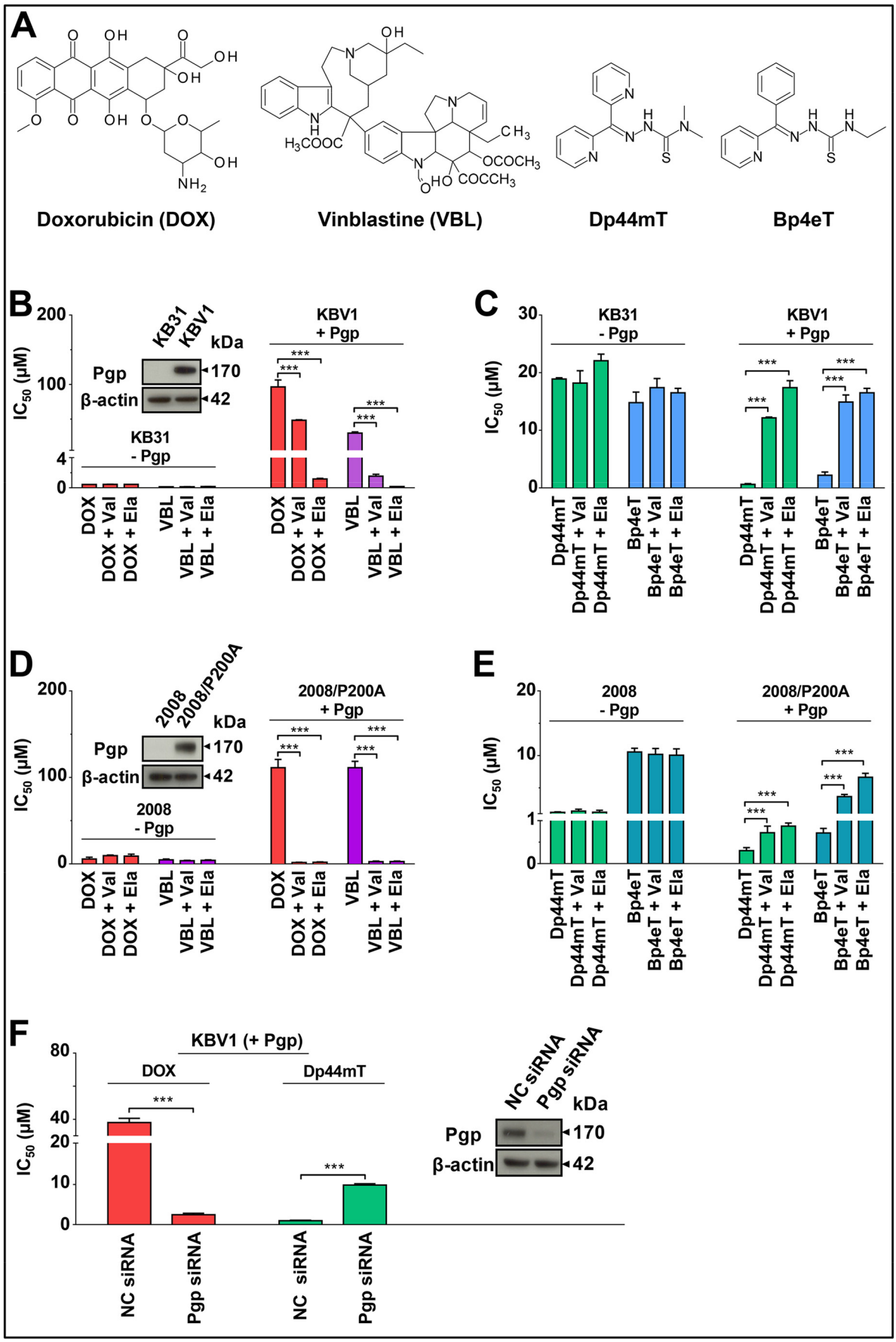
A
Doxorubicin (DOX)
Vinblastine (VBL)
Dp44mT
Bp4eT
B
KB31
KBV1
kDa
Pgp
β-actin
170
42
KB31
- Pgp
KBV1
+ Pgp
IC50 (μM)
DOX
DOX + Val
DOX + Ela
VBL
VBL + Val
VBL + Ela
C
KB31
- Pgp
KBV1
+ Pgp
Dp44mT
Dp44mT + Val
Dp44mT + Ela
Bp4eT
Bp4eT + Val
Bp4eT + Ela
D
2008
2008/P200A
2008
- Pgp
2008/P200A
+ Pgp
E
2008
- Pgp
2008/P200A
+ Pgp
F
KBV1 (+ Pgp)
DOX
Dp44mT
NC siRNA
Pgp siRNA
kDa
Pgp
β-actin
170
42

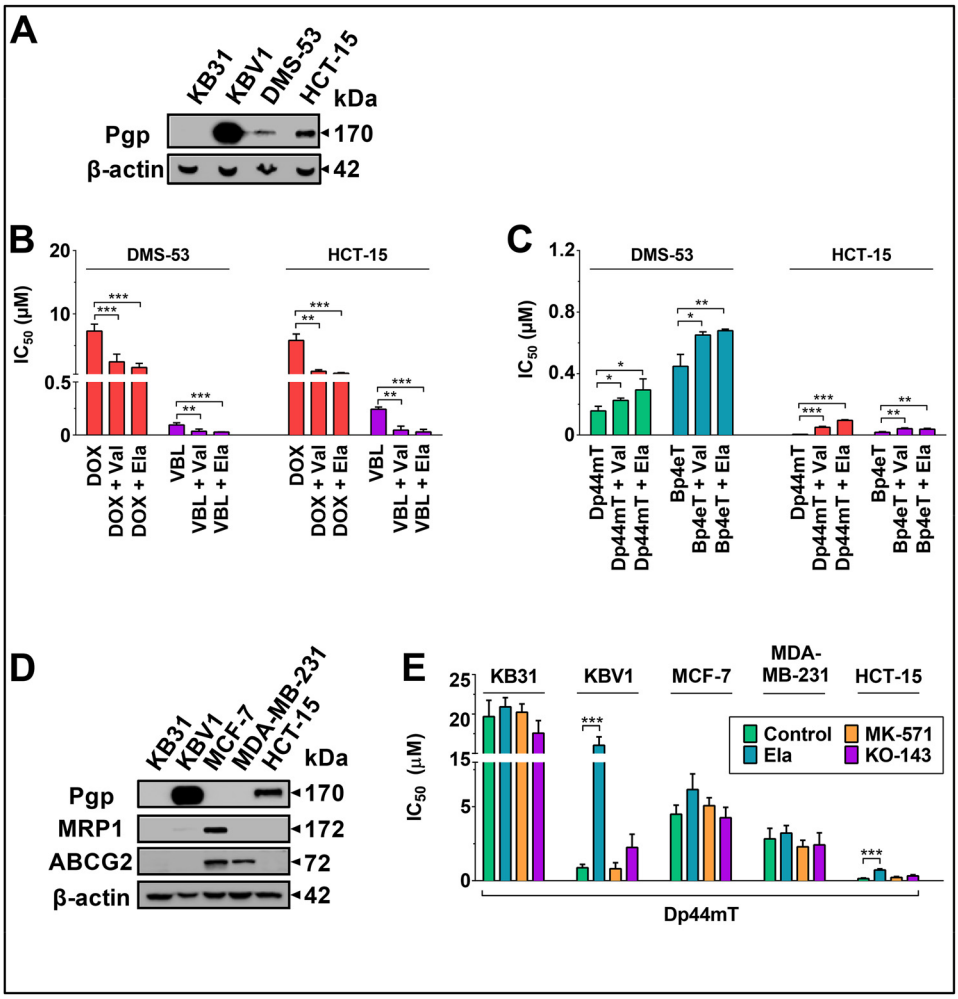

FIGURE 2. **Dp44mT and Bp4eT potentiate cytotoxicity in endogenously Pgp-expressing cells.** *A*, Western blot analysis of Pgp expression in KB31 (−Pgp), KBV1 (+Pgp), DMS-53, and HCT-15 cells. β-Actin was used as a loading control. *B*, Pgp confers resistance to DOX and VBL (IC_{50}/72 h) but can be sensitized in the presence of Pgp inhibitors Val (1 μM) and Ela (0.1 μM) in endogenously Pgp-expressing DMS-53 and HCT-15 cells. *C*, Dp44mT and Bp4eT exert potentiated cytotoxicity to endogenously Pgp-expressing DMS-53 and HCT-15 cells and can be desensitized in the presence of the Pgp inhibitors Val and Ela. *D*, Western blot showing Pgp, MRP1, or ABCG2 expression in KB31, KBV1, MCF-7, MDA-MB-231, and HCT-15 cells. *E*, cellular proliferation studies (MTT assay) measuring the IC_{50} of Dp44mT over a 24-h incubation with KBV1, KB31, MCF-7, MDA-MB-231, and HCT-15 cells. Cells were treated with control medium, the Pgp inhibitor Ela (0.2 μM), the MRP1 inhibitor MK-571 (20 μM), or the ABCG2 inhibitor KO-143 (2 μM). The results are means ± S.D. of three experiments. *, $p < 0.05$; **, $p < 0.01$; ***, $p < 0.001$ *versus* control.

(Fig. 3*A*). Similarly to verapamil, Dp44mT and Bp4eT and their iron and copper complexes (*i.e.* Fe[Dp44mT]$_2$, an iron complex of di-2-pyridylketone 4,4-dimethyl-3-thiosemicarbazone; Cu-[Dp44mT], a copper complex of di-2-pyridylketone 4,4-dimethyl-3-thiosemicarbazone; Fe[Bp4eT]$_2$, an iron complex of 2-benzoylpyridine 4-ethyl-3-thiosemicarbazone; and Cu[Bp4eT], a copper complex of 2-benzoylpyridine 4-ethyl-3-thiosemicarbazone), significantly ($p < 0.001$) stimulated the basal catalytic activity of Pgp (Fig. 3*A*). The cytotoxicity assays (Figs. 1, *C* and *E*, and 2*C*) and Pgp-ATPase activity (Fig. 3*A*) showed similar results for Bp4eT and Dp44mT, but considering the greater cytotoxic activity of Dp44mT in Pgp-expressing cells, it was used in further studies.

To further assess the interaction of Dp44mT with Pgp, the radiolabeled ligand, [^{14}C]Dp44mT, was implemented to determine its uptake and efflux by KBV1 (+Pgp) and KB31 (−Pgp) cells (Fig. 3, *B–E*). The levels of [^{14}C]Dp44mT and known Pgp substrates, [^{14}C]DOX and [^{3}H]VBL (3), were significantly ($p <$ 0.001) decreased in KBV1 (+Pgp) cells *versus* KB31 cells (−Pgp cells; Fig. 3, *B* and *C*). This observation was consistent with

FIGURE 1. **Dp44mT and Bp4eT potentiate cytotoxicity in multidrug-resistant Pgp-expressing cells.** *A*, structures of DOX, VBL, Dp44mT, and Bp4eT. *B*, Pgp confers resistance to DOX and VBL (IC_{50}/72 h) but can be sensitized in the presence of Pgp inhibitors Val (1 μM) and Ela (0.1 μM) in Pgp-expressing KBV1 cells, but not KB31 cells (−Pgp). *Inset*, Western blot of Pgp expression in KBV1 cells (+Pgp) and KB31 cells (−Pgp). *C*, Dp44mT and Bp4eT exert potentiated cytotoxicity to Pgp-expressing KBV1 cells and can be desensitized in the presence of Pgp inhibitors Val and Ela, whereas no effect was observed in KB31 cells (−Pgp). *D*, Pgp confers resistance to DOX and VBL but can be sensitized by the Pgp inhibitors Val and Ela only in Pgp-expressing 2008/P200A cells, but not 2008 cells (−Pgp). *Inset*, Western blot of Pgp expression in 2008/P200 cells (+Pgp) and 2008 cells (−Pgp). *E*, Dp44mT and Bp4eT demonstrate potentiated cytotoxicity in Pgp-expressing 2008/P200A cells and can be desensitized in the presence of Pgp inhibitors Val and Ela (IC_{50}/24 h), whereas no effect was observed in 2008 cells (−*Pgp*). *F*, transient Pgp silencing using siRNA increases DOX cytotoxicity (IC_{50}/72 h) while desensitizing Dp44mT cytotoxicity (IC_{50}/24 h). *Inset*, Western blot showing Pgp-protein expression after silencing with Pgp-siRNA compared with negative control (*NC*) siRNA-treated KBV1 cells. The results are means ± S.D. (three experiments). ***, $p < 0.001$ *versus* control.

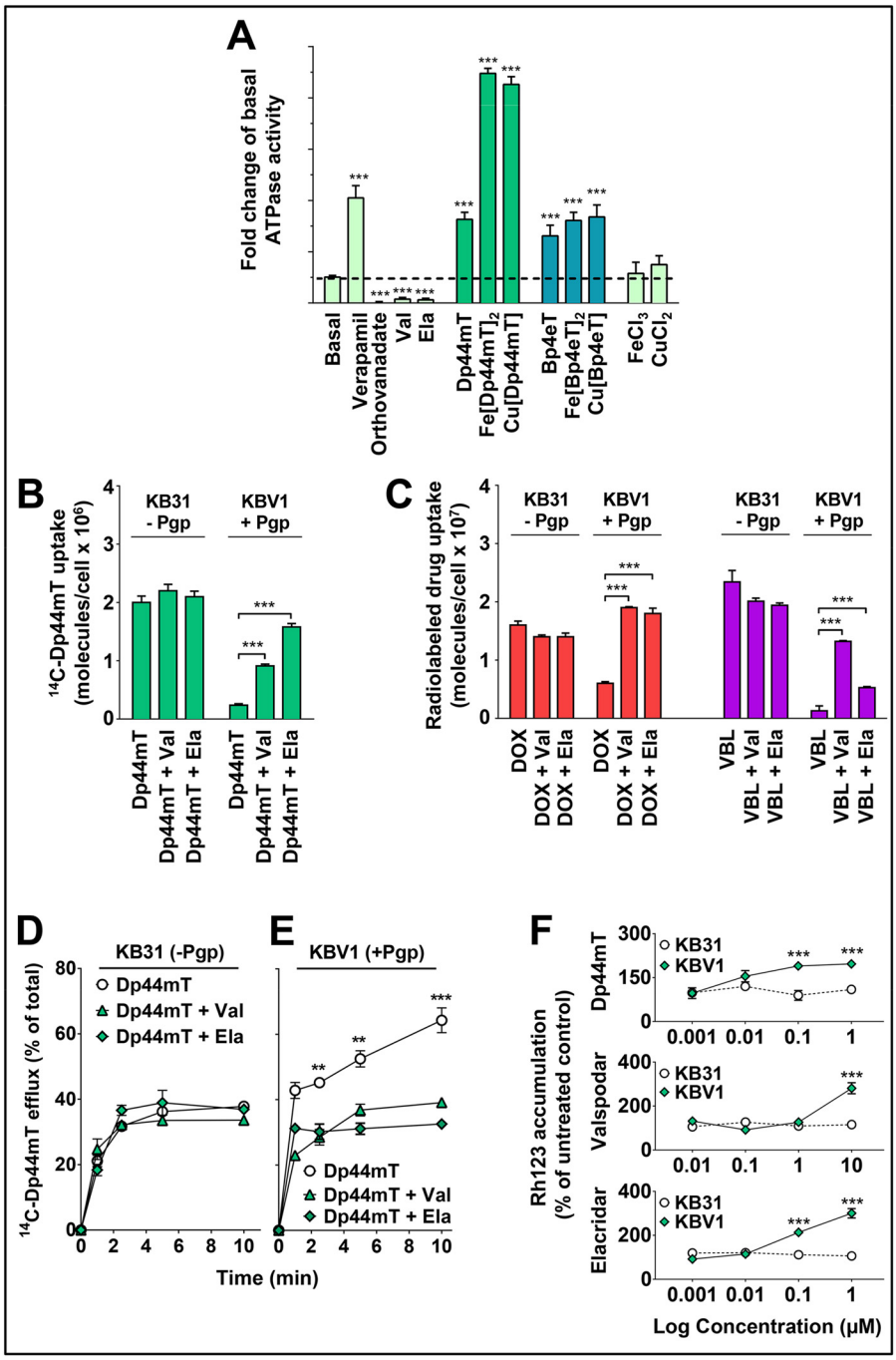

FIGURE 3. **The Dp44mT and Bp4eT ligands and their iron and copper complexes are Pgp substrates.** *A*, Pgp-mediated ATPase activity induced by compounds relative to basal activity by the untreated controls. The well characterized Pgp substrate, verapamil, was used as a positive control, whereas orthovanadate, Val, and Ela were used as inhibitors of Pgp activity (negative controls). The thiosemicarbazones Dp44mT and Bp4eT and their Fe(III) and Cu(II) complexes were examined, and $FeCl_3$ and $CuCl_2$ were used as controls because they were used to prepare the iron and copper complexes of these ligands. *B*, the Pgp inhibitors Val and Ela increase [^{14}C]Dp44mT (1 μCi/ml) uptake by KBV1 cells (+Pgp), but not KB31 cells (−Pgp) after 30 min at 37 °C. *C*, as found for [^{14}C]Dp44mT, Val and Ela increase [^{14}C]DOX (1 μCi/ml) and [^{3}H]VBL (1 μCi/ml) uptake by KBV1 cells (+Pgp), but not KB31 cells (−Pgp) after 30 min at 37 °C. *D*, Pgp inhibitors do not significantly affect [^{14}C]Dp44mT efflux from KB31 cells (−Pgp). *E*, in contrast to *D*, Pgp inhibitors repress [^{14}C]Dp44mT efflux from KBV1 cells (+Pgp). *F*, Dp44mT increases Rh123 retention after a 30-min incubation at 37 °C with KBV1 cells (+Pgp) and acts similarly to the Pgp inhibitors Val and Ela, whereas no effect was observed using KB31 cells (−Pgp). The results are means ± S.D. (three experiments). **, $p < 0.01$; ***, $p < 0.001$ *versus* control.

increased Pgp-mediated efflux of [^{14}C]Dp44mT, [^{14}C]DOX, and [^{3}H]VBL from KBV1 cells. In contrast, the Pgp inhibitors Val and Ela significantly ($p < 0.001$) increased the uptake of [^{14}C]Dp44mT, [^{14}C]DOX, and [^{3}H]VBL in Pgp-expressing KBV1 cells, but not non-Pgp-expressing KB31 cells (Fig. 3, *B* and *C*). Consistent with this finding, significantly ($p < 0.001$) higher efflux of [^{14}C]Dp44mT was observed in KBV1 (+Pgp) cells relative to KB31 cells (−*Pgp*; Fig. 3, *D* and *E*), whereas the Pgp inhibitors Val and Ela significantly ($p < 0.01$–0.001) suppressed [^{14}C]Dp44mT efflux only in Pgp-expressing KBV1 cells (Fig. 3*E*). Collectively, these studies indicated Dp44mT acted as a Pgp substrate.

Dp44mT Competes with a Well Characterized Pgp Substrate to Inhibit Pgp Transport—Because some Pgp substrates are competitive Pgp inhibitors (33, 34), we assessed whether Dp44mT competes with the fluorescent Pgp substrate Rh123 (35) for efflux from cells. As the Dp44mT concentration increased to 0.1 μM or above, Rh123 retention was significantly ($p < 0.001$) increased in KBV1 (+Pgp) cells but not KB31 (−Pgp) cells (Fig. 3*F*). Similarly, the Pgp inhibitors Val and Ela also significantly ($p < 0.001$) increased Rh123 retention in KBV1 cells, but not KB31 cells (Fig. 3*F*). The higher potency of Ela compared with Val, in terms of inhibiting Pgp, is consistent with their affinity for Pgp (18). Taken together, results from Fig. 3 (*A*–*F*) demonstrate that Dp44mT acts as a Pgp substrate and competes for transport with other known substrates.

Pgp Sequesters Dp44mT into Lysosomes to Potentiate Its Damage—Dp44mT targets lysosomes, and after binding intralysosomal Cu (to form the Cu[Dp44mT] complex), it generates ROS to cause LMP (13). Moreover, we showed that lysosomal membrane-bound Pgp transports Pgp substrates, such as DOX (Fig. 1*A*), into this organelle (17). Hence, the potentiating effect of facilitating Dp44mT transport into lysosomes via Pgp was crucial to investigate.

First, in these studies, fluorescence microscopy was used to demonstrate that Pgp (green) was present not only on the cell surface, but it also co-localized (Mander's overlap coefficient (36) of 0.996) with intracellular LAMP2-stained lysosomes (red), in KBV1 cells (+*Pgp*; Fig. 4*A*). Importantly, similar co-localization between Pgp and LAMP2 was also observed with another anti-Pgp antibody (1:100, catalog no. P7965; Sigma) and Texas Red-conjugated secondary antibody (1:1000, catalog no. sc-2781; Santa Cruz Biotechnology).

Next, lysosomal membrane stability was investigated by examining release of the classical lysosomal marker, LysoTracker® Red (37), from damaged lysosomes of KBV1 and KB31 cells. The Cu[Dp44mT] complex was initially examined as it: accumulates in lysosomes (13); causes rapid LMP (within 30 min (13)); and is an avid Pgp substrate (Fig. 3*A*). Under control conditions, the classical punctate pattern of LysoTracker® Red-stained lysosomes (37) in KBV1 (+Pgp) cells was observed (Fig. 4*B*, *panel (i)*). However, after a 30-min incubation with the Cu[Dp44mT] complex, the lysosomal pattern disappeared (Fig. 4*B*, *panel (ii)*), which is consistent with LMP and the release of LysoTracker® Red from lysosomes. Importantly, LMP-induced by Cu[Dp44mT] in KBV1 (+Pgp) cells (Fig. 4*B*, *panel (ii)*) could be prevented by both Pgp inhibitors Val and Ela (Fig. 4*B*, *panels (iii)* and *(iv)*) and was not induced by the relative control, $CuCl_2$ (Fig. 4*B*, *panel (v)*). In contrast to these results, Cu[Dp44mT] did not cause LMP in KB31 cells (−*Pgp*) under all conditions (Fig. 4*B*, *panels (vii)–(ix)*) relative to KB31 cells incubated with control medium (Fig. 4*B*, *panel (vi)*) or $CuCl_2$ only (Fig. 4*B*, *panel (x)*).

Notably, the well characterized Pgp inhibitors Val and Ela do not induce lysosomotropism in KB31 (−Pgp) and KBV1 (+Pgp) cells, because no change in size of the cell (forward scatter) or granularity (side scatter) can be observed with these inhibitors in our flow cytometry studies (17). Hence, under the conditions implemented in this investigation, Val and Ela inhibited Pgp without exhibiting lysosomotropic properties that could have reduced accumulation of Dp44mT in lysosomes. Therefore, these data indicate that inhibiting Pgp transport activity in KBV1 cells blocked Cu[Dp44mT]-mediated uptake and subsequent lysosomal damage, although it had no effect on non-Pgp-expressing KB31 cells (Fig. 4*B*).

Flow cytometric studies using another classical lysosomal marker, acridine orange (13), also demonstrated that LMP induced by Cu[Dp44mT] was Pgp-dependent because the Pgp inhibitor Val significantly ($p < 0.001$) prevented LMP in Pgp-expressing KBV1 cells, but not KB31 (−Pgp) cells (Fig. 4*C*). Notably, $Fe[Dp44mT]_2$ did not affect LMP after a 30-min incubation because of its lower redox activity (13). The Pgp-potentiated LMP was also demonstrated after 24 h with the ligand alone (*i.e.* Dp44mT) because the Pgp inhibitor Val significantly ($p < 0.001$) prevented LMP in KBV1 (+Pgp) cells, but not KB31 (−Pgp) cells (Fig. 4*D*). The delayed LMP by Dp44mT compared with Cu[Dp44mT] could be explained by the facts that Cu[Dp44mT] was a better substrate than Dp44mT alone (Fig. 3*A*), and in contrast to the preformed Cu[Dp44mT] complex, Dp44mT would need to bind copper released from copper-containing proteins catabolized in the lysosome before redox activity could be initiated.

The possibility that Pgp inhibitors directly prevent Cu[Dp44mT]-induced lysosomal damage by inhibiting ROS generation was excluded through control experiments. Indeed, Val or Ela did not prevent the redox activity of Cu[Dp44mT] under lysosomal-like conditions *in vitro* (Fig. 4*E*). In contrast, the Cu chelator, tetrathiomolybdate (Fig. 4*E*), totally prevented Cu[Dp44mT] ROS generation (Fig. 4*E*). These results indicate that Val and Ela do not directly prevent ROS generation and that their ability to prevent Dp44mT or Cu[Dp44mT]-mediated LMP was due to their ability to inhibit Pgp.

Pgp-potentiated Dp44mT Cytotoxicity Is Lysosome-dependent—Considering Dp44mT is a Pgp substrate (Fig. 3), that becomes charged at a lysosomal pH of 5 (13), we examined whether Pgp increases the uptake and trapping of [^{14}C]-Dp44mT in lysosomes. The lysosomotropic weak bases, NH_4Cl, CLQ, or MA (38–40), that increase lysosomal pH (39, 40) were used to prevent the lysosomal trapping of [^{14}C]Dp44mT. All lysosomotropic weak bases significantly ($p < 0.001$) decreased the Pgp-dependent [^{14}C]Dp44mT accumulation in cells (Fig. 4*F*) by neutralizing lysosomal pH, allowing neutral Dp44mT to escape from the organelle, preventing lysosomal damage.

To examine whether lysosomal Pgp (17) and lysosomal trapping of Cu[Dp44mT] or Dp44mT (13) leads to potentiated cytotoxicity, we again disrupted the capability of Cu[Dp44mT] or Dp44mT to be trapped in lysosomes by increasing lysosomal pH using NH_4Cl, CLQ, or MA (17, 41) (Fig. 4, *G* and *H*). The lysosomotropic weak bases significantly ($p < 0.001$) desensitized KBV1 Pgp-expressing cells to Cu[Dp44mT] and Dp44mT after 2 and 24 h of incubation, respectively, but not their non-Pgp-expressing KB31 counterparts (Fig. 4, *G* and *H*).

Lysosomal Trapping of Dp44mT Induces LMP—To investigate the importance of lysosomal trapping of Cu[Dp44mT] in the induction of LMP, the intracellular distribution of the lysosomal enzyme, cathepsin D (13, 42), and its association with lysosomal-associated membrane protein marker, LAMP2 (42),

was studied with fluorescence microscopy (Fig. 5, *A–G*). Control KBV1 (+Pgp) cells stained with LAMP2 (*red*) and cathepsin D (*green*) became co-localized upon the merge, leading to yellow punctate fluorescence consistent with intact lysosomes (Fig. 5*A*). After a 30-min incubation with Cu[Dp44mT], the green punctate fluorescence of cathepsin D was markedly reduced in Pgp-expressing cells, because cathepsin D was released from this organelle (Fig. 5*B*). In contrast, LAMP2 fluorescence was unaffected, probably because LAMP2 is an integral protein of lysosomal membranes (43) and, unlike cathepsin D, cannot freely diffuse out of the lysosome. Quantitation of cathepsin D intensity demonstrated a significant ($p < 0.001$)

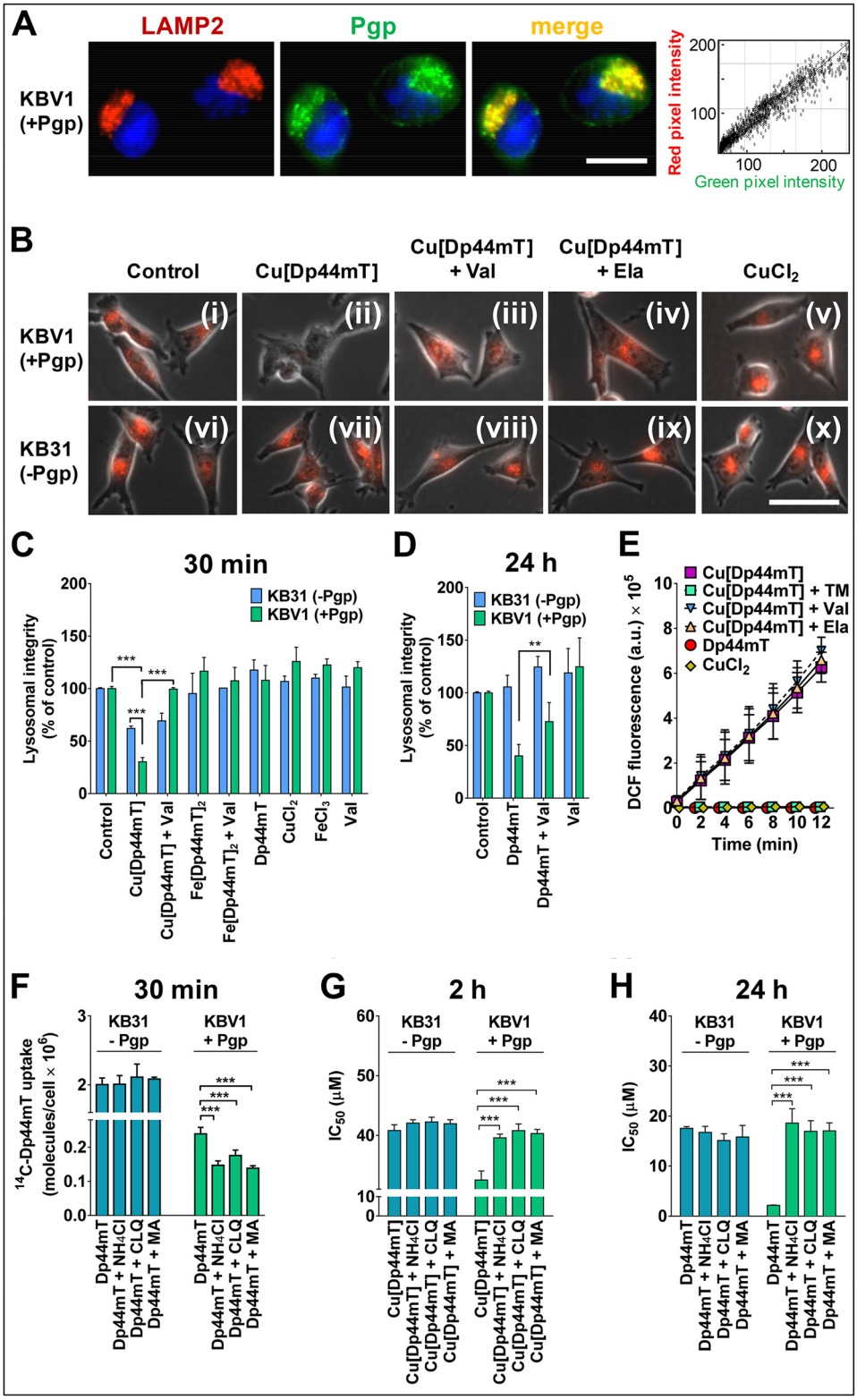

decrease upon Cu[Dp44mT] treatment relative to control KBV1 cells (Fig. 5*G*), consistent with Cu[Dp44mT]-induced LMP (Fig. 4, *B* and *C*). However, cells incubated with Cu[Dp44mT] in the presence of the lysosomotropic weak base, CLQ, demonstrated that the LAMP2 and cathepsin D markers were co-localized, leading to a yellow punctate pattern consistent with undamaged lysosomes that retained cathepsin D (Fig. 5*C*). Quantitation of cathepsin D intensity demonstrated that the addition of CLQ to Cu[Dp44mT] treatment completely prevented the loss in lysosomal fluorescence observed with Cu[Dp44mT] alone in KBV1 cells (Fig. 5*G*).

In contrast, no alteration in the punctate fluorescence of LAMP2 and cathepsin D was observed after incubation of KB31 (−Pgp) cells with Cu[Dp44mT] or Cu[Dp44mT]/CLQ treatment (Fig. 5, *D–G*). Collectively, these results in Figs. 4 and 5 demonstrate that Dp44mT and Cu[Dp44mT] require Pgp for lysosomal accumulation and also an acidic lysosomal pH for trapping to enhance cytotoxicity in Pgp-expressing cells via LMP.

Dp44mT Markedly Targets Pgp-expressing Tumors in Vivo—To examine whether Dp44mT (administered intravenously (tail vein); 5 days/week) targets human Pgp-expressing tumors more effectively than their non-Pgp-expressing counterparts, we utilized BALB/c nu/nu mice subcutaneously injected with KBV1 (+Pgp) or KB31 (−Pgp) cells on the left and right flanks of the same mouse, respectively (Fig. 6*A*). Treatment began after the tumor reached 120 mm^3 (9). After 9 days of treatment, in mice receiving the vehicle control, both the KBV1 (+Pgp) and KB31 (−Pgp) tumors grew linearly as a function of time ($r = 0.93$ and 0.92, respectively), reaching 632 ± 63% and 894 ± 104% of the initial tumor volume (day 0), respectively (Fig. 6, *B* and *C*). Because tumor size in the vehicle control group approached the maximum limit (1000 mm^3) prescribed by the local animal ethics committee, it was not possible to continue the study past day 9.

Notably, Dp44mT was significantly ($p < 0.001$) more effective at inhibiting the net growth of KBV1 (+Pgp) tumor xenografts relative to KB31 (−Pgp) tumor xenografts when comparisons were made after 4, 7, and 9 days of growth (Fig. 6, *B* and *C*). Dp44mT (0.1 or 0.2 mg/kg) reduced tumor growth by 9–10-fold in KBV1 (+Pgp) xenografts relative to the vehicle control (Fig. 6*B*), whereas a 1.7–1.8-fold reduction in tumor growth was observed in KB31 (−Pgp) tumors compared with the vehicle control group (Fig. 6*C*). Throughout the treatment time course with Dp44mT or the vehicle control, there was no significant ($p > 0.05$) alteration in the body weight of mice bearing KBV1 or KB31 tumors (Fig. 6*D*), as shown previously (9). The representative tumor size on day 9 (Fig. 6*E*) clearly demonstrated that Dp44mT (0.1 or 0.2 mg/kg/day) was far more efficient in inhibiting tumor growth in Pgp-expressing KBV1 tumors than in non-Pgp-expressing KB31 tumors.

Immunohistochemistry demonstrated that Pgp expression in KBV1 tumors was maintained in mice treated for 9 days, whereas no Pgp was detected in KB31 tumors (Fig. 6*F*). Importantly, Pgp expression in KBV1 (+Pgp) tumors was markedly reduced upon treatment with Dp44mT at 0.1 or 0.2 mg/kg, suggesting killing of Pgp-expressing tumor cells. As a negative control, we also used an IgG isotype control antibody (IgG; Fig. 6*G*) from a nonimmunized rabbit to match the concentration of the primary Pgp antibody. This control demonstrated that the staining observed in KBV1 cells was specific for Pgp. In summary, this *in vivo* study highlights the potent activity of Dp44mT against Pgp-expressing tumors.

DISCUSSION

MDR is a major obstacle for cancer treatment (1, 2), and there is a critical need for the development of alternative treatments and agents that can overcome resistance. Moreover, attempts over many decades to develop agents that overcome resistance have not been successful in the clinics (1, 2, 44).

Herein, we demonstrate for the first time how the new anticancer agent, Dp44mT, overcomes multidrug resistance through utilization of the lysosomal drug transporter, Pgp, resulting in enhanced cytotoxicity to the resistant tumor cell. In this case, Dp44mT is transported into the lysosome by Pgp where it induces increased anti-tumor activity (via LMP) and overcomes drug resistance. Notably, this property is not found for standard Pgp substrates and depends on the redox activity of the Dp44mT-Cu complex. This effect is in marked contrast and in fact opposite to what occurs with standard chemotherapeutics that are Pgp substrates such as DOX, where Pgp acts to prevent cytotoxicity and results in drug resistance by totally different mechanisms, namely, drug efflux out of the cell and drug storage in the lysosome where the organelle acts as a safe house and prevents the cytotoxic action of the agent (17).

Through the fundamental understanding of the molecular mechanism by which Dp44mT overcomes drug resistance via lysosomal Pgp, this study offers novel insights into the molecular and cellular interactions of these agents that can be specifically utilized to design new drugs that can overcome drug resistance. Hence, agents that target lysosomes offer an exciting new therapeutic strategy to combat MDR via utilization of lysosomal Pgp transport activity.

FIGURE 4. **Pgp-potentiated cytotoxicity by Cu[Dp44mT] and Dp44mT is due to lysosomal damage.** *A*, fluorescence microscopy demonstrating LAMP2-stained lysosomes (*red*) co-localize with Pgp (*green*) in KBV1 cells (+Pgp), leading to *yellow* fluorescence. *B*, *panels (i)–(iv)*, LysoTracker® Red-stained lysosomes in control KBV1 cells (+Pgp) were compromised when incubated (30 min at 37 °C) with Cu[Dp44mT] (*panel (ii)*), but not control medium (*panel (i)*) or $CuCl_2$ (*panel (v)*). In contrast, the Pgp inhibitors Val (*panel (iii)*) and Ela (*panel (iv)*) prevent lysosomal damage by Cu[Dp44mT]. In contrast, examining KB31 cells (−Pgp), Cu[Dp44mT] (*panel (vii)*) has no effect on LysoTracker® Red lysosomal fluorescence in KB31 cells relative to cells incubated with control medium alone (*panel (vi)*). Furthermore, in KB31 cells, addition of Val (*panel (viii)*) or Ela to Cu[Dp44mT] (*panel (ix)*) or $CuCl_2$ (*panel (x)*) has no effect on LysoTracker® Red lysosomal fluorescence. *C* and *D*, flow cytometry indicates that within 30 min (*C*) or 24 h (*D*), lysosomal integrity (judged by acridine orange fluorescence) was compromised to a greater extent in KBV1 cells (+Pgp) relative to KB31 cells (−Pgp) incubated with Cu[Dp44mT] or Dp44mT, respectively. In contrast, lysosomal integrity was maintained by Val in KBV1 cells. *E*, as judged by the DCF assay, Val and Ela do not scavenge Cu[Dp44mT]-induced ROS under lysosomal-like conditions (pH 5.0 and in the presence of cysteine) (13, 59). *F*, the lysosomotropic weak bases, NH_4Cl, CLQ, or MA, decrease [^{14}C]Dp44mT uptake only in KBV1 cells (+Pgp) after 30 min at 37 °C. *G* and *H*, incubation of KB31 (−Pgp) or KBV1 (+Pgp) cells with the lysosomotropic weak bases and either Cu[Dp44mT] for 2 h at 37 °C (*G*) or Dp44mT for 24 h at 37 °C (*H*) decreases Cu[Dp44mT] cytotoxicity in only KBV1 (+Pgp) cells. The results shown in *A* and *B* are from three experiments. *C–H* show means ± S.D. (3–6 experiments). **, $p < 0.01$; ***, $p < 0.001$ *versus* control. *Scale bars*, 50 μm.

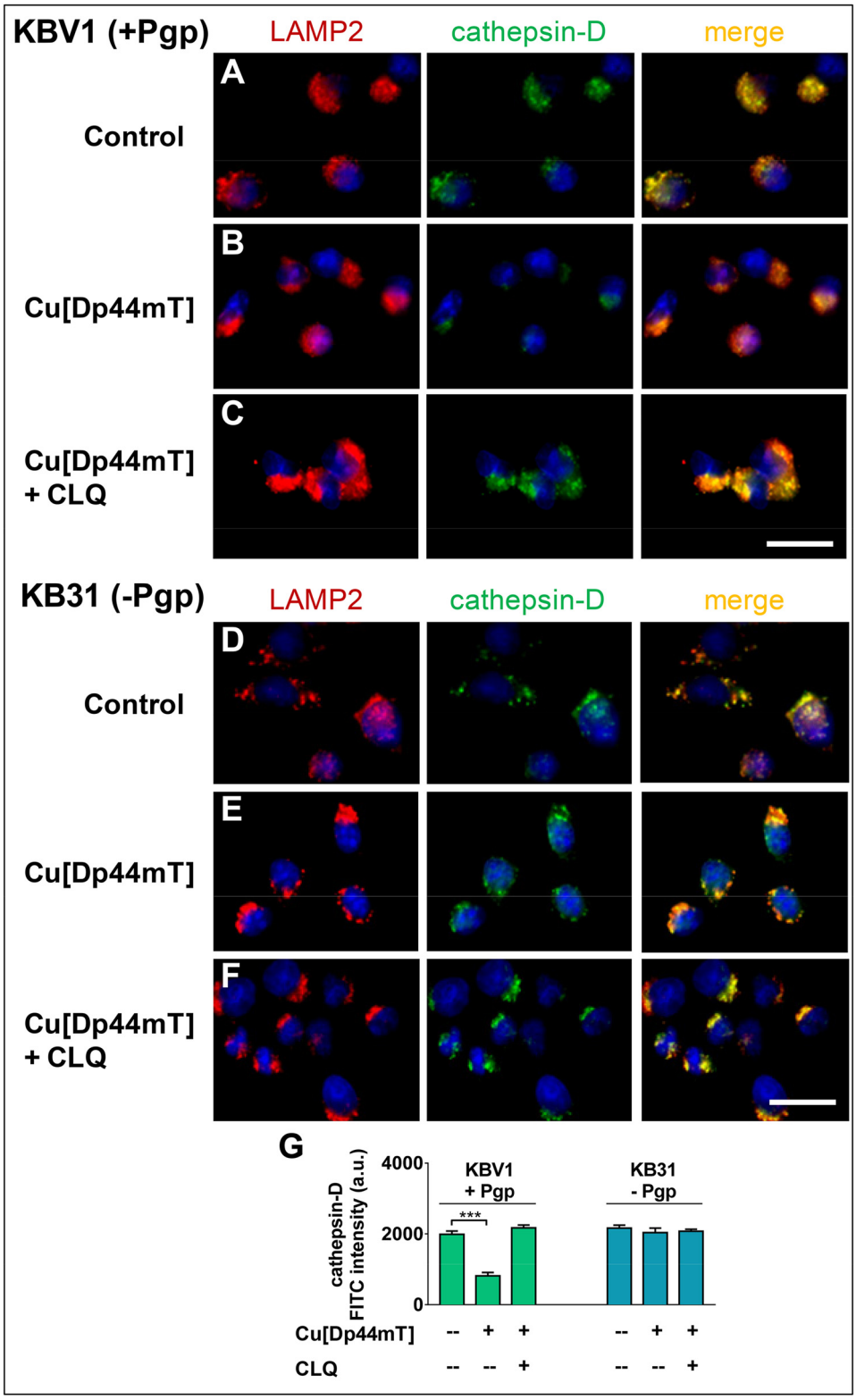

FIGURE 5. **LMP induced by Cu[Dp44mT] can be prevented with the lysosomotropic weak base, CLQ, in Pgp-expressing cells.** *A*, LAMP2 (*red*) and cathepsin D (*green*) in KBV1 cells (+Pgp) co-localize (*yellow* fluorescence) to indicate lysosomes upon the merge. *B*, incubation of KBV1 (+Pgp) cells with Cu[Dp44mT] (25 μM) for 30 min at 37 °C leads to a loss of lysosomal cathepsin D from LAMP2-stained lysosomes, resulting in decreased yellow fluorescence upon the merge. *C*, incubation of KBV1 (+Pgp) cells with Cu[Dp44mT] (25 μM) and CLQ (1 μM) prevents cathepsin D redistribution from LAMP2-stained lysosomes. This lysosomotropic weak base maintains the yellow fluorescence of intact lysosomes. *D–F*, incubation of KB31 (−Pgp) cells with Cu[Dp44mT] or Cu[Dp44mT]/CLQ for 30 min at 37 °C results in no change in LAMP2 and cathepsin D-stained lysosomes, which is consistent with intact lysosomes. *G*, quantitation of cathepsin D intensity in the fluorescence images shown in *A–F*. The images are typical from three experiments, and the results in *G* are means ± S.D. ($n = 3$). *Scale bars*, 50 μm. ***, $p < 0.001$ *versus* untreated.

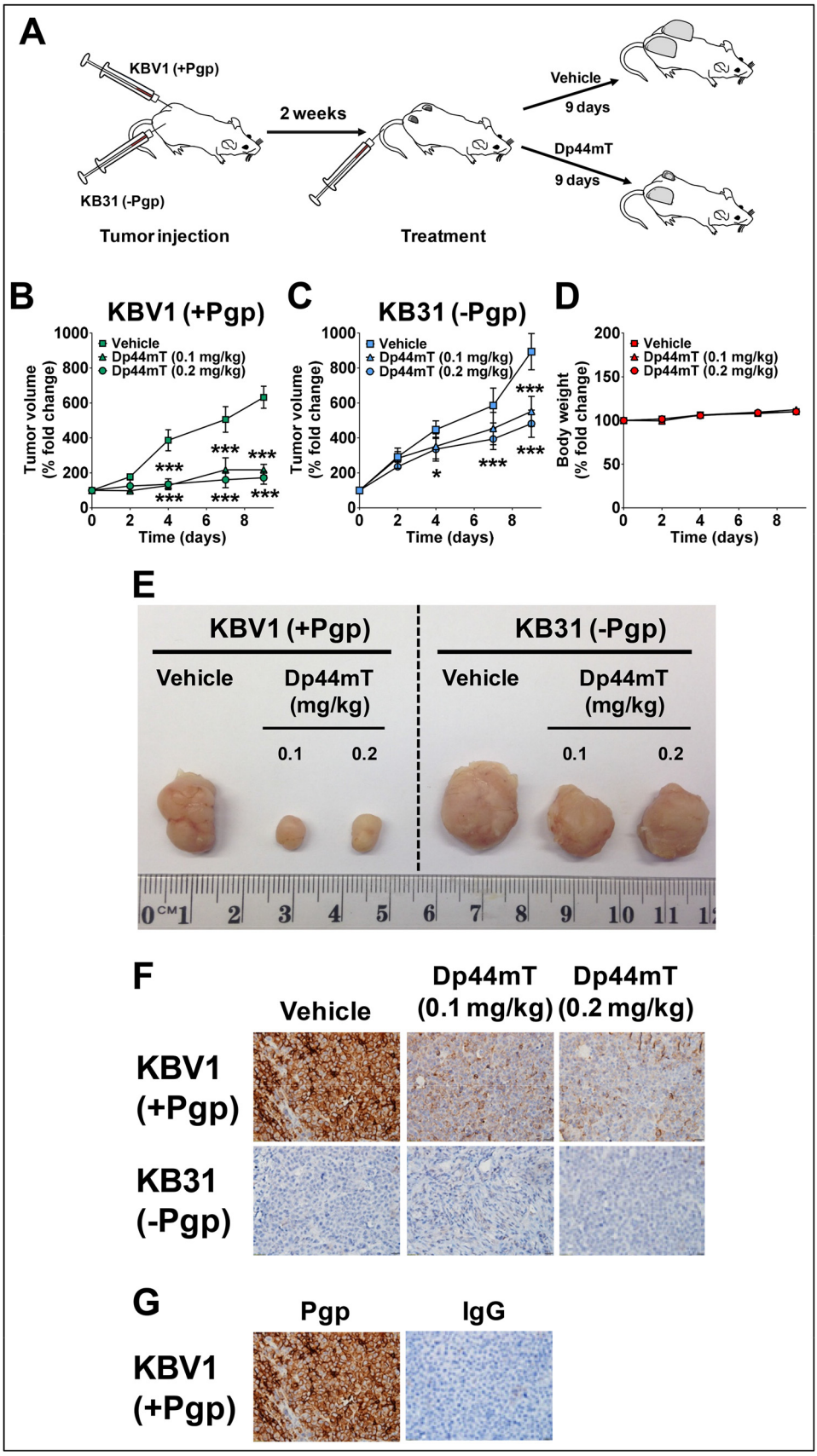
A
KBV1 (+Pgp)
KB31 (-Pgp)
Tumor injection
2 weeks
Treatment
Vehicle
9 days
Dp44mT
9 days
B
KBV1 (+Pgp)
Vehicle
Dp44mT (0.1 mg/kg)
Dp44mT (0.2 mg/kg)
Tumor volume (% fold change)
Time (days)
C
KB31 (-Pgp)
D
Body weight (% fold change)
E
KBV1 (+Pgp)
KB31 (-Pgp)
Vehicle
Dp44mT (mg/kg)
0.1
0.2
F
Vehicle
Dp44mT (0.1 mg/kg)
Dp44mT (0.2 mg/kg)
KBV1 (+Pgp)
KB31 (-Pgp)
G
Pgp
IgG
KBV1 (+Pgp)

In the current study, it is notable that both Pgp inhibitors and siRNA-mediated Pgp silencing were utilized to demonstrate that Pgp was crucial for the potentiated cytotoxicity of Dp44mT toward MDR cells. Moreover, the interaction of Dp44mT with Pgp was also confirmed using three methods: 1) measurement of Pgp-ATPase activity of isolated Pgp-protein; 2) [^{14}C]Dp44mT uptake and efflux studies in the presence and absence of Pgp inhibitors; and 3) competition experiments where increasing Dp44mT concentrations were able to compete for Pgp transport, leading to retention of the Pgp substrate, Rh123. Collectively, these studies demonstrate that Dp44mT is a Pgp substrate (Fig. 3).

As discussed above, despite being a Pgp substrate, Dp44mT behaved oppositely to the classical Pgp substrates, DOX and VBL (3). Indeed, these latter agents were more potent in drug-sensitive, non-Pgp-expressing cells (Fig. 1, *B* and *D*), whereas Dp44mT was more effective in multidrug-resistant Pgp-expressing cells and cells endogenously expressing Pgp (Figs. 1, *C* and *E*, and 2*C*). Furthermore, Pgp inhibitors increased sensitivity to DOX and VBL in Pgp-expressing cells (Figs. 1, *B* and *D*, and 2*B*), although these inhibitors significantly decreased the effect of Dp44mT (Figs. 1, *C* and *E*, and 2*C*). The difference in cytotoxicity between Dp44mT and these classical Pgp substrates was dependent on how these agents interact with lysosomes once transported into this organelle by Pgp. In the case of Dp44mT, it hijacks lysosomal Pgp to increase lysosomal targeting, resulting in LMP (Fig. 4, *B–D*). In contrast, the transport of DOX by Pgp into the lysosome leads to a protective effect, with the lysosome acting to prevent cytotoxicity and resulting in resistance (17). The difference between these Pgp substrates depends upon the interaction with lysosomal copper, with Dp44mT forming a highly redox active copper complex that leads to marked LMP (Figs. 4, *B*, *C*, and *E*; 5; and 7). Hence, incorporating a copper-binding pharmacophore into agents that accumulate in lysosomes offers a new strategy that can be implemented in designing anti-cancer agents for overcoming Pgp-mediated resistance.

Considering our previous studies demonstrating that Dp44mT can be charged and trapped within the acidic lysosome (13), it was hypothesized that raising lysosomal pH with lysosomotropic weak bases (45, 46) could also increase the proportion of the neutral species released from lysosomes without inducing LMP (41, 47). Indeed, incubation of [^{14}C]Dp44mT with three different lysosomotropic weak bases decreased [^{14}C]Dp44mT uptake (Fig. 4*F*), decreased cytotoxicity (Fig. 4, *G* and *H*), and prevented LMP (Fig. 5). These observations were only found in Pgp-expressing cells and not in those without Pgp. This Pgp-mediated transport of Dp44mT increases lysosomal uptake, upon which this agent becomes charged because of the low pH (pH 5) (13), preventing it from escaping lysosomes and enabling it to induce cytotoxicity caused by LMP (Fig. 7). Hence, although Dp44mT is effluxed out of the cell by plasma membrane-Pgp (Figs. 3*E* and 7), the simultaneous

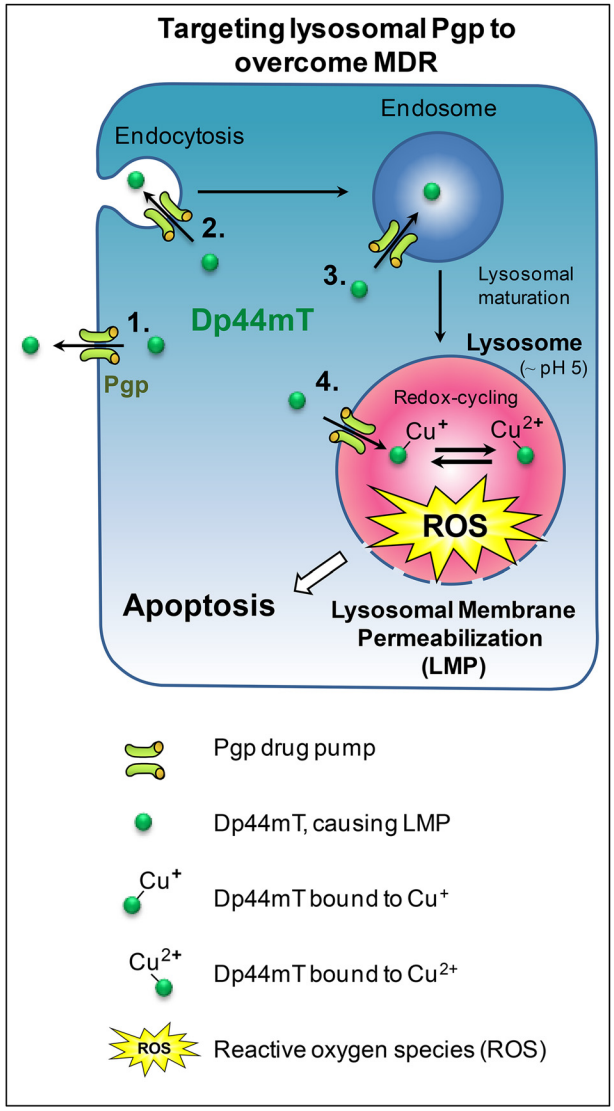

FIGURE 7. **Schematic diagram of the mechanism of Pgp-mediated cytotoxicity by Dp44mT.** *Step 1*, Pgp-localized on the plasma membrane facilitates efflux of substrates such as Dp44mT out of the cell. *Step 2*, as part of endocytosis, Pgp on the plasma membrane "buds" inwards to form early endosomes (60). As a consequence of endocytosis, the topology of Pgp is inverted, as demonstrated for other membrane proteins (61, 62), resulting in substrate transport into the endosome. Thus, Pgp remains functional, because its catalytic active sites and ATP-binding domains still remain exposed in the cytosol (61, 62). *Step 3*, the inversion of Pgp orientation leads to Dp44mT transport into the vesicle lumen. As the endosome matures into a lysosome, it becomes increasingly acidified. *Step 4*, active Pgp-mediated transport of Dp44mT increases lysosomal uptake where it becomes positively charged and trapped because of the acidic lysosomal pH. The Dp44mT then binds copper in lysosomes (which recycle this nutrient during autophagy) to form a potent, redox active complex that generates ROS and causes LMP and apoptosis (15).

FIGURE 6. **Dp44mT targets Pgp-expressing KBV1 tumors *in vivo* to a markedly greater extent than KB31 tumors that do not express Pgp.** *A*, basic experimental protocol used for the mouse tumor model. *B* and *C*, Dp44mT (0.1 or 0.2 mg/kg) was administered intravenously once per day, 5 days/week for up to 9 days to nude mice bearing a VBL-resistant KBV1 (+Pgp) tumor xenograft on the left flank (*B*) and a VBL-sensitive KB31 (−Pgp) human tumor xenograft on the right flank (*C*). Each point represents the mean ± S.E. of tumor volume (% fold change) relative to tumor size at day 0. *D*, body weight of the nude mice treated in *B* and *C*. *E*, photograph of KBV1 (+Pgp) and KB31 (−Pgp) tumors taken from mice after 9 days of treatment using the regimen in *B* and *C*. *F*, immunohistochemistry of Pgp expression from the KBV1 and KB31 tumors shown in *E*. *G*, as an appropriate negative control, an isotype control antibody (IgG) from a nonimmunized rabbit was used at the same concentration of a primary Pgp antibody used on a section of KBV1 (+Pgp) tumor. The results in *B–D* are means ± S.E. ($n = 6$/group). *E* and *F* are typical photographs taken from the vehicle control and treatment groups. *, $p < 0.05$; ***, $p < 0.001$ *versus* control.

enhanced Pgp-mediated, lysosomal accumulation of Dp44mT is critical for mediating LMP and cytotoxicity.

The mechanism of action of Dp44mT involves ROS generation and potent lysosomal damage after binding Cu in Pgp-expressing cells (Figs. 4, *B*, *C*, and *E*, and 5). This finding is significant, because tumor cells relative to their normal counterparts have enhanced metabolism of metals including copper (48). Numerous studies have indicated higher copper levels in cancer patient serum (49) and the tumor relative to normal tissue (50–52). It has also been suggested that because of recycling of cellular constituents via autophagy, lysosomes in tumor cells contain greater quantities of metals including copper (53, 54). Hence, the copper-related mechanism described herein involving lysosomal targeting of thiosemicarbazones via Pgp could explain their well known selectivity against cancer cells *versus* normal cells (8–11, 55, 56). Therefore, ROS-generating agents such as Dp44mT (13, 14) can hijack lysosomal Pgp to selectively overcome drug resistance by inducing more lysosomal damage in Pgp-expressing cells relative to their non-Pgp-expressing counterparts (Fig. 7).

Importantly, Dp44mT was found to selectively target chemotherapeutic-resistant human Pgp-expressing tumors over non-Pgp-expressing human tumors *in vivo* (Fig. 6, *B*, *C*, and *E*). Compared with vehicle-treated control tumors, the efficacy of Dp44mT at reducing tumor growth was >5-fold more in KBV1 (+Pgp) relative to KB31 (−Pgp) xenografts. This result is significant, because attempts to reverse resistance by using MDR modulators have not been successful in clinical trials (4, 5). Hence, the ability of Dp44mT to overcome MDR offers a significant advantage over other chemotherapeutics and the unsuccessful attempts to reverse resistance with MDR modulators (4, 5).

In addition to overcoming MDR, it is well described that DpT thiosemicarbazones also potently inhibit tumor growth and metastasis *in vivo* (9, 11, 12, 57). This latter property is particularly significant, because metastasis is responsible for 90% of cancer deaths (58). Furthermore, the DpT class of thiosemicarbazones is well tolerated *in vivo* (12). These properties, combined with the ability of DpT thiosemicarbazones to overcome MDR, accredits them with unique pharmacological properties for effective cancer therapy.

In conclusion, for the first time, our studies demonstrate a key role for lysosomal Pgp in overcoming drug resistance and offer a mechanism for the potentiated cytotoxicity in MDR cells (9). Moreover, Dp44mT selectively targets chemotherapeutic resistant human Pgp-expressing tumors over non-Pgp-expressing tumors *in vivo*. The sensitizing action of Pgp on Dp44mT-mediated cytotoxicity was dependent on three characteristics of this agent: 1) it must be a Pgp substrate; 2) it has to become charged at acidic pH to enable accumulation in lysosomes; and 3) the agent must cause marked redox stress in the acidic lysosome leading to cytotoxic ROS that induces LMP and cell death. This latter property is not found for other classical Pgp substrates (*e.g.* DOX) that are sequestered in the lysosome, which leads to resistance to the agent (17). Hence, this study offers novel insights into the molecular and cellular interactions of these agents that can be specifically utilized to design new drugs, such as novel thiosemicarbazones, that can overcome drug resistance (9).

Acknowledgments—We acknowledge the Bosch Institute Flow Cytometry Unit and Advanced Microscopy Facility (University of Sydney) for assistance with the Zeiss Axiovision co-localization software.

REFERENCES

1. Leonard, G. D., Fojo, T., and Bates, S. E. (2003) The role of ABC transporters in clinical practice. *Oncologist* **8,** 411–424
2. Higgins, C. F. (2007) Multiple molecular mechanisms for multidrug resistance transporters. *Nature* **446,** 749–757
3. Shen, D. W., Cardarelli, C., Hwang, J., Cornwell, M., Richert, N., Ishii, S., Pastan, I., and Gottesman, M. M. (1986) Multiple drug-resistant human KB carcinoma cells independently selected for high-level resistance to colchicine, adriamycin, or vinblastine show changes in expression of specific proteins. *J. Biol. Chem.* **261,** 7762–7770
4. Akhtar, N., Ahad, A., Khar, R. K., Jaggi, M., Aqil, M., Iqbal, Z., Ahmad, F. J., and Talegaonkar, S. (2011) The emerging role of P-glycoprotein inhibitors in drug delivery: a patent review. *Expert Opin. Ther. Pat.* **21,** 561–576
5. Saneja, A., Khare, V., Alam, N., Dubey, R. D., and Gupta, P. N. (2014) Advances in P-glycoprotein-based approaches for delivering anticancer drugs: pharmacokinetic perspective and clinical relevance. *Expert Opin. Drug Deliv.* **11,** 121–138
6. Heffeter, P., Jakupec, M. A., Körner, W., Chiba, P., Pirker, C., Dornetshuber, R., Elbling, L., Sutterlüty, H., Micksche, M., Keppler, B. K., and Berger, W. (2007) Multidrug-resistant cancer cells are preferential targets of the new antineoplastic lanthanum compound KP772 (FFC24). *Biochem. Pharmacol.* **73,** 1873–1886
7. Ludwig, J. A., Szakács, G., Martin, S. E., Chu, B. F., Cardarelli, C., Sauna, Z. E., Caplen, N. J., Fales, H. M., Ambudkar, S. V., Weinstein, J. N., and Gottesman, M. M. (2006) Selective toxicity of NSC73306 in MDR1-positive cells as a new strategy to circumvent multidrug resistance in cancer. *Cancer Res.* **66,** 4808–4815
8. Yuan, J., Lovejoy, D. B., and Richardson, D. R. (2004) Novel di-2-pyridyl-derived iron chelators with marked and selective antitumor activity: in vitro and in vivo assessment. *Blood* **104,** 1450–1458
9. Whitnall, M., Howard, J., Ponka, P., and Richardson, D. R. (2006) A class of iron chelators with a wide spectrum of potent antitumor activity that overcomes resistance to chemotherapeutics. *Proc. Natl. Acad. Sci. U.S.A.* **103,** 14901–14906
10. Lovejoy, D. B., Sharp, D. M., Seebacher, N., Obeidy, P., Prichard, T., Stefani, C., Basha, M. T., Sharpe, P. C., Jansson, P. J., Kalinowski, D. S., Bernhardt, P. V., and Richardson, D. R. (2012) Novel second-generation di-2-pyridylketone thiosemicarbazones show synergism with standard chemotherapeutics and demonstrate potent activity against lung cancer xenografts after oral and intravenous administration *in vivo*. *J. Med. Chem.* **55,** 7230–7244
11. Liu, W., Xing, F., Iiizumi-Gairani, M., Okuda, H., Watabe, M., Pai, S. K., Pandey, P. R., Hirota, S., Kobayashi, A., Mo, Y. Y., Fukuda, K., Li, Y., and Watabe, K. (2012) N-myc downstream regulated gene 1 modulates Wnt-β-catenin signalling and pleiotropically suppresses metastasis. *EMBO Mol. Med.* **4,** 93–108
12. Kovacevic, Z., Chikhani, S., Lovejoy, D. B., and Richardson, D. R. (2011) Novel thiosemicarbazone iron chelators induce up-regulation and phosphorylation of the metastasis suppressor N-myc down-stream regulated gene 1: a new strategy for the treatment of pancreatic cancer. *Mol. Pharmacol.* **80,** 598–609
13. Lovejoy, D. B., Jansson, P. J., Brunk, U. T., Wong, J., Ponka, P., and Richardson, D. R. (2011) Antitumor activity of metal-chelating compound Dp44mT is mediated by formation of a redox-active copper complex that accumulates in lysosomes. *Cancer Res.* **71,** 5871–5880
14. Jansson, P. J., Sharpe, P. C., Bernhardt, P. V., and Richardson, D. R. (2010) Novel thiosemicarbazones of the ApT and DpT series and their copper complexes: identification of pronounced redox activity and characterization of their antitumor activity. *J. Med. Chem.* **53,** 5759–5769

15. Richardson, D. R., Sharpe, P. C., Lovejoy, D. B., Senaratne, D., Kalinowski, D. S., Islam, M., and Bernhardt, P. V. (2006) Dipyridyl thiosemicarbazone chelators with potent and selective antitumor activity form iron complexes with redox activity. *J. Med. Chem.* **49,** 6510–6521
16. Kalinowski, D. S., Yu, Y., Sharpe, P. C., Islam, M., Liao, Y. T., Lovejoy, D. B., Kumar, N., Bernhardt, P. V., and Richardson, D. R. (2007) Design, synthesis, and characterization of novel iron chelators: structure-activity relationships of the 2-benzoylpyridine thiosemicarbazone series and their 3-nitrobenzoyl analogues as potent antitumor agents. *J. Med. Chem.* **50,** 3716–3729
17. Yamagishi, T., Sahni, S., Sharp, D. M., Arvind, A., Jansson, P. J., and Richardson, D. R. (2013) P-Glycoprotein mediates drug resistance via a novel mechanism involving lysosomal sequestration. *J. Biol. Chem.* **288,** 31761–31771
18. Bihorel, S., Camenisch, G., Lemaire, M., and Scherrmann, J. M. (2007) Modulation of the brain distribution of imatinib and its metabolites in mice by valspodar, zosuquidar and elacridar. *Pharm. Res.* **24,** 1720–1728
19. Ogihara, T., Kamiya, M., Ozawa, M., Fujita, T., Yamamoto, A., Yamashita, S., Ohnishi, S., and Isomura, Y. (2006) What kinds of substrates show P-glycoprotein-dependent intestinal absorption? Comparison of verapamil with vinblastine. *Drug Metab. Pharmacokinet.* **21,** 238–244
20. Ivanova, S., Repnik, U., Bojic, L., Petelin, A., Turk, V., and Turk, B. (2008) Chapter nine lysosomes in apoptosis. *Methods Enzymol.* **442,** 183–199
21. Lee, Y., Lee, C., and Yoon, J. (2004) Kinetics and mechanisms of DMSO (dimethylsulfoxide) degradation by UV/H_2O_2 process. *Water Res.* **38,** 2579–2588
22. McGrath, J. C., Drummond, G. B., McLachlan, E. M., Kilkenny, C., and Wainwright, C. L. (2010) Guidelines for reporting experiments involving animals: the ARRIVE guidelines. *Br. J. Pharmacol.* **160,** 1573–1576
23. Murphy, L., Henry, M., Meleady, P., Clynes, M., and Keenan, J. (2008) Proteomic investigation of taxol and taxotere resistance and invasiveness in a squamous lung carcinoma cell line. *Biochim. Biophys. Acta* **1784,** 1184–1191
24. Boquete, A. L., Vargas Roig, L., López, G. A., Gude, R., Binda, M. M., González, A. D., Ciocca, D. R., and Bonfil, R. D. (2001) Differential anthracycline sensitivity in two related human colon carcinoma cell lines expressing similar levels of P-glycoprotein. *Cancer Lett.* **165,** 111–116
25. Cole, S. P., Bhardwaj, G., Gerlach, J. H., Mackie, J. E., Grant, C. E., Almquist, K. C., Stewart, A. J., Kurz, E. U., Duncan, A. M., and Deeley, R. G. (1992) Overexpression of a transporter gene in a multidrug-resistant human lung cancer cell line. *Science* **258,** 1650–1654
26. Doyle, L. A., Yang, W., Abruzzo, L. V., Krogmann, T., Gao, Y., Rishi, A. K., and Ross, D. D. (1998) A multidrug resistance transporter from human MCF-7 breast cancer cells. *Proc. Natl. Acad. Sci. U.S.A.* **95,** 15665–15670
27. Sharom, F. J. (2008) ABC multidrug transporters: structure, function and role in chemoresistance. *Pharmacogenomics* **9,** 105–127
28. Ansbro, M. R., Shukla, S., Ambudkar, S. V., Yuspa, S. H., and Li, L. (2013) Screening compounds with a novel high-throughput ABCB1-mediated efflux assay identifies drugs with known therapeutic targets at risk for multidrug resistance interference. *PLoS One* **8,** e60334
29. Morrow, C. S., Peklak-Scott, C., Bishwokarma, B., Kute, T. E., Smitherman, P. K., and Townsend, A. J. (2006) Multidrug resistance protein 1 (MRP1, ABCC1) mediates resistance to mitoxantrone via glutathione-dependent drug efflux. *Mol. Pharmacol.* **69,** 1499–1505
30. Kalalinia, F., Elahian, F., Mosaffa, F., and Behravan, J. (2014) Celecoxib up regulates the expression of drug efflux transporter ABCG2 in breast cancer cell lines. *Iran J. Pharm. Res.* **13,** 1393–1401
31. Watts, R. N., Hawkins, C., Ponka, P., and Richardson, D. R. (2006) Nitrogen monoxide (NO)-mediated iron release from cells is linked to NO-induced glutathione efflux via multidrug resistance-associated protein 1. *Proc. Natl. Acad. Sci. U.S.A.* **103,** 7670–7675
32. Allen, J. D., van Loevezijn, A., Lakhai, J. M., van der Valk, M., van Tellingen, O., Reid, G., Schellens, J. H., Koomen, G. J., and Schinkel, A. H. (2002) Potent and specific inhibition of the breast cancer resistance protein multidrug transporter in vitro and in mouse intestine by a novel analogue of fumitremorgin C. *Mol. Cancer Ther.* **1,** 417–425
33. Urbatsch, I. L., al-Shawi, M. K., and Senior, A. E. (1994) Characterization of the ATPase activity of purified Chinese hamster P-glycoprotein. *Biochemistry* **33,** 7069–7076
34. Schinkel, A. H., and Jonker, J. W. (2003) Mammalian drug efflux transporters of the ATP binding cassette (ABC) family: an overview. *Adv. Drug Deliv. Rev.* **55,** 3–29
35. Pilarski, L. M., Szczepek, A. J., and Belch, A. R. (1997) Deficient drug transporter function of bone marrow-localized and leukemic plasma cells in multiple myeloma. *Blood* **90,** 3751–3759
36. Bolte, S., and Cordelières, F. P. (2006) A guided tour into subcellular colocalization analysis in light microscopy. *J. Microsc.* **224,** 213–232
37. Chazotte, B. (2011) Labeling lysosomes in live cells with LysoTracker. *Cold Spring Harb. Protoc.* **2011,** pii
38. Agostinelli, E., and Seiler, N. (2007) Lysosomotropic compounds and spermine enzymatic oxidation products in cancer therapy (review). *Int. J. Oncol.* **31,** 473–484
39. de Duve, C., de Barsy, T., Poole, B., Trouet, A., Tulkens, P., and Van Hoof, F. (1974) Lysosomotropic agents. *Biochem. Pharmacol.* **23,** 2495–2531
40. Bharadwaj, S., Rathore, S. S., and Ghosh, P. C. (2006) Enhancement of the cytotoxicity of liposomal ricin by the carboxylic ionophore monensin and the lysosomotropic amine NH_4Cl in Chinese hamster ovary cells. *Int. J. Toxicol.* **25,** 349–359
41. Antoine, J. C., Goud, B., Jouanne, C., Maurice, M., and Feldmann, G. (1985) Ammonium chloride, methylamine and chloroquine reversibly inhibit antibody secretion by plasma cells. *Biol. Cell* **55,** 41–54
42. Yelamanchili, S. V., Chaudhuri, A. D., Flynn, C. T., and Fox, H. S. (2011) Upregulation of cathepsin D in the caudate nucleus of primates with experimental parkinsonism. *Mol. Neurodegener.* **6,** 52
43. Eskelinen, E. L. (2006) Roles of LAMP-1 and LAMP-2 in lysosome biogenesis and autophagy. *Mol. Aspects Med.* **27,** 495–502
44. Choi, Y. H., and Yu, A. M. (2014) ABC transporters in multidrug resistance and pharmacokinetics, and strategies for drug development. *Curr. Pharm. Des.* **20,** 793–807
45. Styrt, B., and Klempner, M. S. (1986) Inhibition of neutrophil oxidative metabolism by lysosomotropic weak bases. *Blood* **67,** 334–342
46. Xiong, S., Li, H., Yu, B., Wu, J., and Lee, R. J. (2010) Triggering liposomal drug release with a lysosomotropic agent. *J. Pharm. Sci.* **99,** 5011–5018
47. Altan, N., Chen, Y., Schindler, M., and Simon, S. M. (1998) Defective acidification in human breast tumor cells and implications for chemotherapy. *J. Exp. Med.* **187,** 1583–1598
48. Gupte, A., and Mumper, R. J. (2009) Elevated copper and oxidative stress in cancer cells as a target for cancer treatment. *Cancer Treat. Rev.* **35,** 32–46
49. Habib, F. K., Dembinski, T. C., and Stitch, S. R. (1980) The zinc and copper content of blood leucocytes and plasma from patients with benign and malignant prostates. *Clin. Chim. Acta* **104,** 329–335
50. Sapota, A., Darago, A., Taczalski, J., and Kilanowicz, A. (2009) Disturbed homeostasis of zinc and other essential elements in the prostate gland dependent on the character of pathological lesions. *Biometals* **22,** 1041–1049
51. Guntupalli, J. N., Padala, S., Gummuluri, A. V., Muktineni, R. K., Byreddy, S. R., Sreerama, L., Kedarisetti, P. C., Angalakuduru, D. P., Satti, B. R., Venkatathri, V., Pullela, V. B., and Gavarasana, S. (2007) Trace elemental analysis of normal, benign hypertrophic and cancerous tissues of the prostate gland using the particle-induced X-ray emission technique. *Eur. J. Cancer Prev.* **16,** 108–115
52. Banas, A., Kwiatek, W. M., Banas, K., Gajda, M., Pawlicki, B., and Cichocki, T. (2010) Correlation of concentrations of selected trace elements with Gleason grade of prostate tissues. *J. Biol. Inorg. Chem.* **15,** 1147–1155
53. van den Berghe, P. V., Folmer, D. E., Malingré, H. E., van Beurden, E., Klomp, A. E., van de Sluis, B., Merkx, M., Berger, R., and Klomp, L. W. (2007) Human copper transporter 2 is localized in late endosomes and lysosomes and facilitates cellular copper uptake. *Biochem. J.* **407,** 49–59
54. Yu, Z., Eaton, J. W., and Persson, H. L. (2003) The radioprotective agent, amifostine, suppresses the reactivity of intralysosomal iron. *Redox. Rep.* **8,** 347–355
55. Rao, V. A., Klein, S. R., Agama, K. K., Toyoda, E., Adachi, N., Pommier, Y., and Shacter, E. B. (2009) The iron chelator Dp44mT causes DNA damage and selective inhibition of topoisomerase IIalpha in breast cancer cells. *Cancer Res.* **69,** 948–957

56. Yu, Y., Suryo Rahmanto, Y., and Richardson, D. R. (2012) Bp44mT: an orally active iron chelator of the thiosemicarbazone class with potent anti-tumour efficacy. *Br. J. Pharmacol.* **165,** 148–166
57. Chen, Z., Zhang, D., Yue, F., Zheng, M., Kovacevic, Z., and Richardson, D. R. (2012) The iron chelators Dp44mT and DFO inhibit TGF-β-induced epithelial-mesenchymal transition via up-regulation of N-Myc downstream-regulated gene 1 (NDRG1). *J. Biol. Chem.* **287,** 17016–17028
58. Hanahan, D., and Weinberg, R. A. (2000) The hallmarks of cancer. *Cell* **100,** 57–70
59. Pisoni, R. L., Acker, T. L., Lisowski, K. M., Lemons, R. M., and Thoene, J. G. (1990) A cysteine-specific lysosomal transport system provides a major route for the delivery of thiol to human fibroblast lysosomes: possible role in supporting lysosomal proteolysis. *J. Cell Biol.* **110,** 327–335
60. Mukherjee, S., Ghosh, R. N., and Maxfield, F. R. (1997) Endocytosis. *Physiol. Rev.* **77,** 759–803
61. Sarkadi, B., Price, E. M., Boucher, R. C., Germann, U. A., and Scarborough, G. A. (1992) Expression of the human multidrug resistance cDNA in insect cells generates a high activity drug-stimulated membrane ATPase. *J. Biol. Chem.* **267,** 4854–4858
62. Shapiro, A. B., and Ling, V. (1994) ATPase activity of purified and reconstituted P-glycoprotein from Chinese hamster ovary cells. *J. Biol. Chem.* **269,** 3745–3754